Int. J. Electrochem. Sci., 11 **(2016)** 8546 – 8560, doi: 10.20964/2016.10.20

International Journal of ELECTROCHEMICAL SCIENCE
www.electrochemsci.org

Electrochemical Detection of Nitrofuranzone and its Metabolite Using Glassy Carbon Electrode Modified by Fe_3O_4 Functionalized Graphene

Baoshan He[*], *Gengan Du*

School of Food Science and Technology, Henan University of Technology, Zhengzhou 450001, People's Republic of China
[*]E-mail: hebaoshan@126.com

Received: 8 July 2016 / *Accepted:* 17 August 2016 / *Published:* 6 September 2016

A new electrochemical sensor that designed by using a glassy carbon electrode modified with graphene and Fe_3O_4 nanoparticles (Gr/Fe_3O_4/GCE) was used to detect nitrofuranzone and semicarbazide hydrochloride. The successful synthesis of composite materials Fe_3O_4 functionalized grapheme overcame the aggregation on the surface of GCE successfully and performed higher catalytic activity, reduced the interfacial resistance, and made the electron transfer easier. Under the optimal conditions, the obtained sensor presented linear response to nitrofuranzone in the range of 1.0×10^{-5} to 1.09×10^{-4} mol/L, the linear regression equation was i_{pc} (10^{-6}A)=-0.0219c (10^{-6}mol/L)-3.5303 with linear correlation coefficient was 0.9815. The detection limit was 2.92×10^{-6}. The linear range of semicarbazide hydrochloride was 1.0×10^{-6} to 1.09×10^{-4} mol/L and the linear regression equation was i_{pa} (10^{-6}A)=0.0240c (10^{-6}mol/L)+0.7497 with linear correlation coefficient was 0.9992. The detection limit was 6.17×10^{-7} mol/L. The recovery rate of nitrofuranzone and semicarbazide hydrochloride was 80.8%~86% and 83.4%~86.1%, respectively.

Keywords: Electrochemical detection; Nitrofuranzone; Semicarbazide hydrochloride; Fe_3O_4 functionalized graphene; Glassy carbon electrode

1. INTRODUCTION

Nitrofurazone, as well as a synthetic broad-spectrum antibiotics, has been largely applied in the treatment and prevention of various bacterial diseases and protozoan infections caused by Escherichia coli and Salmonella spp[1-2]. It is belongs to the nitroufuran group of antibiotics, mainly including nitrofurazone, nitrofurantoin, furazolidone and furaltadone. In addition to their function as effective growth promoters, nitrofurans are also used to largely enhance the productivity of farm animals and

aquatic organisms[3]. But in the long-term study in laboratory, the people find that nitrofurans and their metabolites have chronic toxicity. A strong drug toxicity reaction caused by long-term or high-dose use the drugs, which main manifestations are hemolytic anemia, thrombopenia, insanity, increased eosinophils and other allergic reactions[4-5]. Because of their potentially carcinogenic and mutagenic effects on human health, many countries have banned the use of such drugs and set up strict inspection standards for their residues in poultry, aquatic products and other animal products.

Nitrofurazone is metabolized in vivo within a few hours and is unlikely to detect the parental drug, so it is inappropriate to detect the parent drug directly[6]. However, the metabolite of it can form a stable compound with the protein in the tissue, which can be kept for a long time in the tissue. Thus, the measuring of its bound metabolite of semicarbazide (SEM) can achieve the monitoring of illegal use of nitrofurazone.

At present, the method for detecting nitrofurazone and its metabolite mainly uses high performance liquid chromatography, liquid chromatography-tandem mass spectrometry, liquid chromatography-mass spectrometry and UV spectrophotometry[7-14]. These methods require large instruments, long testing time and the general laboratory can't meet the requirements. Moreover, they need to be derived and cannot meet the field testing and large sample detection. Compared with the above methods, electrochemical detecting has advantages as portable device, sensitive and rapid[14-18]. Graphene, a novel two dimensional (2D) carbonaceous material, is composed offree-standing carbon atoms which are densely packed into a six-angle type honeycomb crystal structure possessing superb thermal conductivity, excellent electrocatalytic activity and fast charge mobility.

Therefore, it can be used as an ideal electrode modification material[19-20]. Magnetite Fe_3O_4 nanocomposites with strong super-paramagnetic nature, low-toxicity and high conductivity[21-23]. However, pure magnetite nanoparticles are easy to accumulate. Therefore, in order to exert both of their superiorities sufficiently, we construct a composite material consisting of graphene and Fe_3O_4 that shows good magnetic properties, high catalytic activity and well electron transfer ability as well as prevent the heavy aggregation[24-25].

Based on these facts, the composite material, namely Gr/Fe_3O_4, was pretreated by using the direct reaction of graphene oxide and ferrous sulfate. The as-prepared Gr/Fe_3O_4 nanocomposites are used to construct modified electrodes (Gr/Fe_3O_4/GCE) for rapid detecting nitrofurazone and semicarbazide hydrochloride (Due to the poor stability of semicarbazide existing alone, it was usually add hydrochloric acid to generate semicarbazide hydrochloride). The fabricated electrode exhibits favorable selectivity, simplicity and sensitivity to detect in real samples.

2. EXPERIMENTAL

2.1. Reagents and Instruments

Graphene was provided from Ningbo Institute of Industrial Technology. Nitrofurazone (NF) were purchased from Shanghai source leaf Biological Technology Co., Ltd. (Shanghai, China). and semicarbazide hydrochloride (SEM·HCL) were purchased from Thermo Fisher Scientific (China) Co.,

Ltd. (Shanghai, China).Sulfate heptahydrate ($FeSO_4·7H_2O$, 99%~101%), sulphuric acid (H_2SO_4, 98%), hydrogen peroxide (H_2O_2, 30%) and sodium hydroxide (NaOH, ≥96%) were supplied by Luoyang Chemical Reagent Factory (Luoyang,China). All other chemicals were of analytical grade and used without further purification.

Cyclic voltammetry (CV), electrochemical impedance spectroscopy (EIS), and amperometric i-t curve (i-t) were carried out using a CHI660E electrochemical workstation (Shanghai ChenHua Instrument Company, china). All electrochemical experiments were performed with a conventional three-electrode system, where the modified GCE as working electrode, the saturated calomel electrode as the reference electrode, the platinum wire as the counter electrode. Fourier Transform infrared spectroscopy was carried out on Nicolet 6700 (Thermo Fisher Scientific, america) and transmission electron microscope (TEM) was carried out on HT7700 (Hitachi, japan).

2.2. Preparation of Gr/ Fe_3O_4 nanocomposites

At first, graphene oxide (GO) was synthesized by the Hummers method with the graphene as raw material[26]. 20 mg graphene oxide was dissolved in 100mL double distilled water under ultrasound for 20 minutes. Then, odium hydroxide was used to adjust pH to 11 or 12. Next, after added 0.8224 g ferrous sulfate and 5 mL hydrazine hydrate, stirring and ultrasonic for 15 minutes. Later, the beaker was sealed by plastic film and putted in the vacuum drying oven at 100 ℃ temperatures. Finally, the black colour solution was cooled and washed three times with double distilled water to get neutral. The treated materials was filtrated by a vacuum pump and dried in a vacuum oven at 60℃

2.3. Fabrication of the working electrode

Prior to each modification, the surface of bare GCE was successively polished on a circular polishing pad with 1.0, 0.3, 0.05 μm graininess Al_2O_3 emulsion, and then sonicated by using acetone, double distilled water sequentially. 3 mg Gr/Fe_3O_4 was added into 2 mL DMF and then ultrasound for 1h to get a homogeneous suspension. 2μL of the Gr/Fe_3O_4 suspension was dropped on the surface of a bare GCE and dried at room temperature. Graphene modified electrodes were made by the same procedure.

3. RESULTS AND DISCUSSION

3.1. TEM Characterization of Gr/Fe_3O_4 nanocomposites

The surface of Gr modified electrode and Gr/Fe_3O_4 modified electrode was investigated by transmission electron microscopy (TEM), as shown in the Figure 1. In figure (a), the characteristics of graphene of transparent thin-layer was very noticeable and the structure of graphene is relatively complete. It was obviously that graphene had slightly folded structure. The synthesis pathway of Gr/Fe_3O_4 used the strong oxidizing of graphene oxide oxidized bivalent iron ions into trivalent iron

ions and ultimately in-situ deposition of Fe_3O_4 nanoparticles. Meanwhile, graphene oxide was reduced to graphene. One step synthesis of composite was used to obtain Gr/Fe_3O_4 nanocomposites. As shown in figure (b), most of the irregular spherical shape Fe_3O_4 particles uniformly distributed on the surface of graphene.

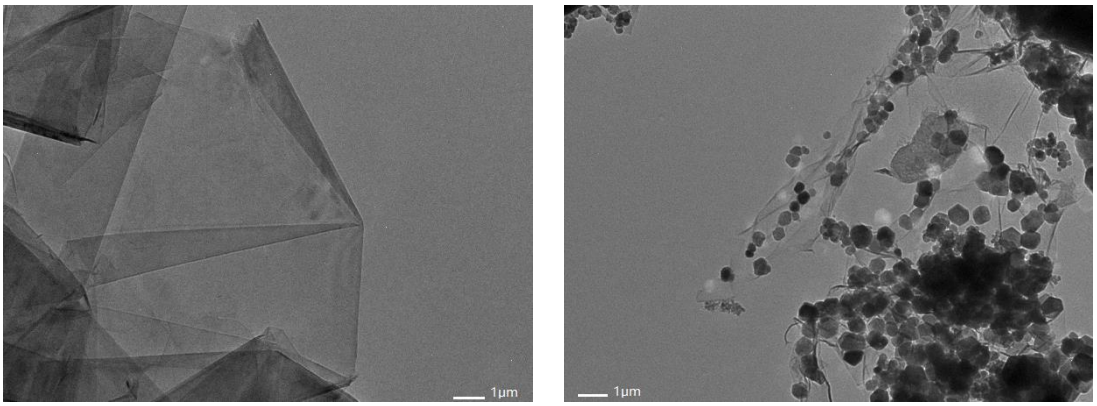

Figure 1. TEM image of (a) Gr and (b) Gr/Fe_3O_4.

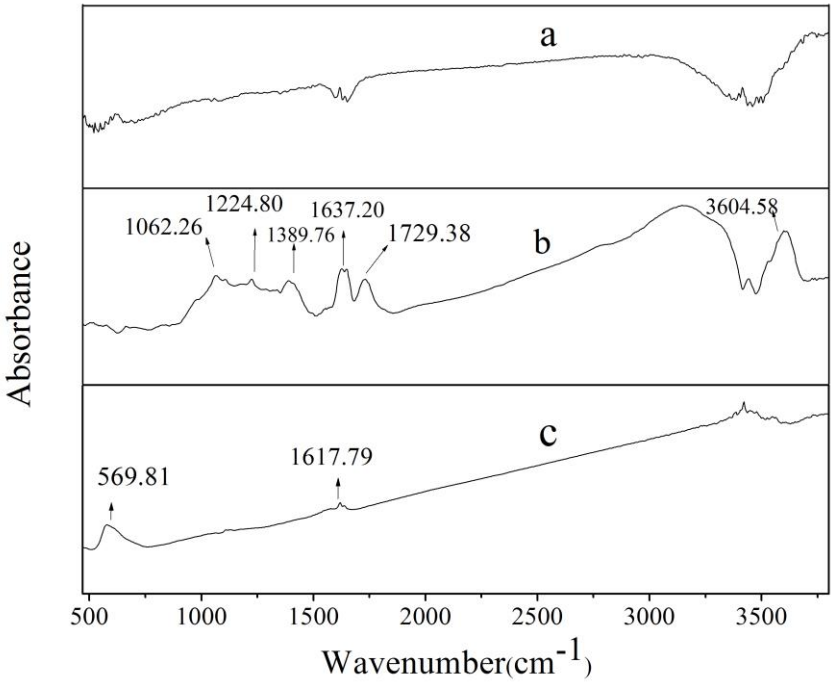

Figure 2. FT-IR curves of (a) Gr, (b) GO and (c) Gr/Fe_3O_4.

But there was a slight agglomeration. Fe_3O_4 particles could effectively alleviate the accumulation of graphene, increase the distance between the graphene sheets, so that the electrochemical ability to get better. These results are similar to those of previous literatures [27-29].

3.2. FT-IR Characterization of Gr/Fe3O4 nanocomposites

Compared with the FT-IR curves of graphene and graphene oxide, it can be found that the FT-IR curve of graphene oxide appears several absorption peaks related to oxygen: the absorption peak at 1062.26 cm^{-1} was the C-O-C stretching vibration of epoxy group. The peak at 1224.80 cm^{-1} was the C-OH stretching vibration. The peaks at 1389.76 cm^{-1} and 1637.20 cm^{-1} correspond to the bending vibration and stretching vibration of –OH, respectively. The peak at 1720 cm^{-1} was the stretching vibration of C=O and the peak at 3604 cm^{-1} was the stretching vibration of O-H, which indicated that there existed carboxyl groups in graphene oxide. From this, graphene oxide had epoxy groups, hydroxyl and carboxyl. Then, the infrared curve of Gr/Fe_3O_4 has changed a great change, there was a strong absorption peak at 569.81 cm^{-1}, corresponding to the Fe-O bond stretching vibration of Fe_3O_4, indicating the successful generation of Fe_3O_4 on graphene. The disappearance of the characteristic peaks of 1729.38 cm^{-1} and 1224.80 cm^{-1} showed that the carboxyl and hydroxyl groups of the oxidized graphene were reduced by hydrazine hydrate. These results are similar to those of previous literatures[30-31].

3.3. Electrochemical impedance spectroscopy of the electrode

Electrochemical impedance spectroscopy (EIS) was used to characterize the interface properties of the modification of the electrode.

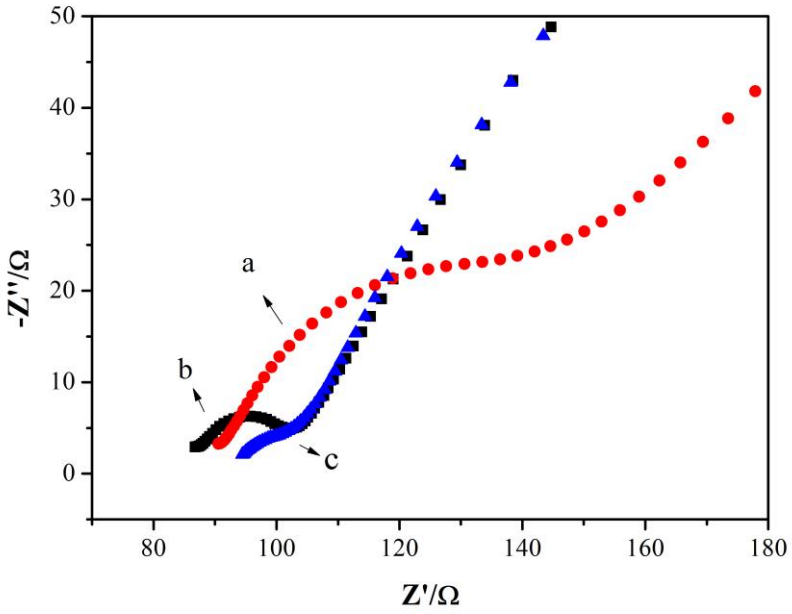

Figure 3. Nyquist plot for faradaic impedance measurements in a solution containing 10mM $[Fe(CN)_6]^{3-/4-}$ and 0.10 M KCL:(a) bare GCE,(b) Gr/GCE,(c) Gr/Fe_3O_4/GCE.

As shown in Figure 3.the electron transfer resisitance (Rct) at bare GCE can be estimated to be about 45 Ω (a). By comparing with the graphene modified electrode (15 Ω), a significant decrease was

observed (b). After modified Gr/Fe_3O_4, the Rct decrease to 6 Ω, indicating the improvement in the conductivity, which provides more electron conduction pathways between the electrode and electrolyte. Based on these results, it may be speculated that the best electrochemical behavior should be the Gr/Fe_3O_4/GCE. This may be attributed to the larger surface area and good conductivity of the Gr/Fe_3O_4 nanocomposites. The results were consistent with that in previous reports [21, 29].

3.4. Electrochemical response of nitrofurazone and semicarbazide hydrochloride

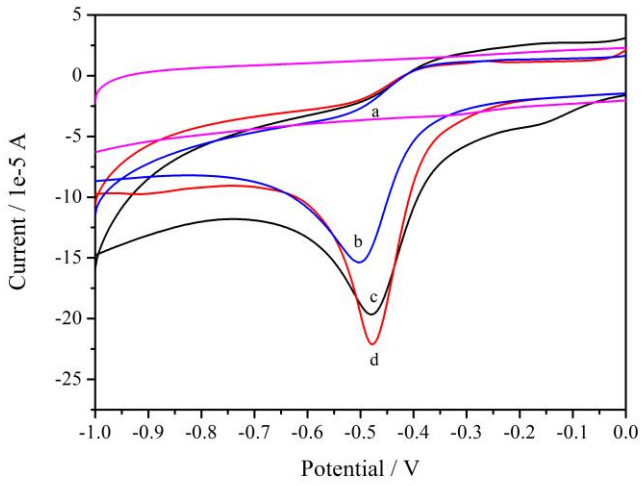

Figure 4. Cyclic voltammetry of (a) bare GCE in the absence of nitrofurazone, (b) bare GCE, (c) Gr/GCE and (d) Gr/Fe_3O_4/GCE in the presence of 2×10^{-4} mol/L nitrofurazone in 1M Hac-NaAc buffering solution (pH6.0).

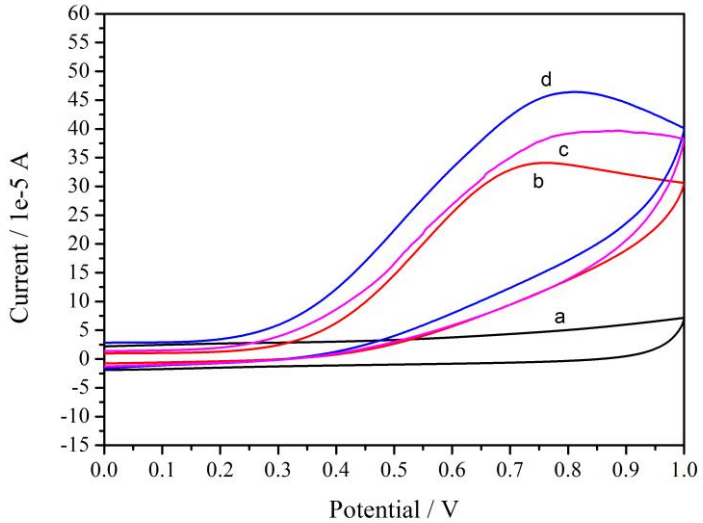

Figure 5. Cyclic voltammetry of (a) bare GCE in the absence of semicarbazide hydrochloride, (b) bare GCE, (c) Gr/GCE and (d) Gr/Fe_3O_4/GCE in the presence of 1×10^{-2} mol/L semicarbazide hydrochloride in 1M Hac-NaAc buffering solution (pH6.0)

As shown in Figure 4 and Figure 5, the electrochemical behavior of three different modified electrodes in 1M Hac-NaAc buffering solution (pH6.0) was investigated by cyclic voltammetric technique at a scan rate of 100 mV/s.

First, we can see from Figure 4 there is no cathodic peak in absence of nitrofurazone (a). When there was 2×10^{-4} nitrofurazone in buffer solution, a reduction peak current appeared at around -0.5 v at bare GCE (b). At Gr/GCE, An obvious increase peak appeared (c) and for Gr/Fe_3O_4/GCE, the reduction peak current was increased remarkably and the reduction peak potentials were shifted a little positively. Among the three modified electrodes, the Gr/Fe_3O_4/GCE displayed a better electrochemical performance towards the reduction of nitrofurazone. The cathodic peak current for nitorfurazonge electroreduction using the Gr/Fe_3O_4/GCE was almost 1.5 times higher than that of bare GCE. Then, similar situation can be seen from Figure 5, An oxidation peak appears at around 0.72 v in the presence of 1×10^{-2} mol/L semicarbazide hydrochloride at bare and compared no semicarbazide hydrochloride existed, there was no oxidation peak presented under the same potential. It is worth noting that Gr/Fe_3O_4/GCE shows good electrocatalytic activity toward semicarbazide hydrochloride oxidation process. It is also almost 1.5 times higher than that of bare GCE, when using the Gr/Fe_3O_4/GCE performed cyclic voltammetry experiment. All of the above results manifested graphene is an excellent support material and acts an effective electron promoter for electrocatalytic reduction of nitrofurazone and oxidation of semicarbazide hydrochloride. The existence of Fe_3O_4 nanoparticles provided good synergistic effects to enhance the conductive area and electron transfer rate between target objects and electrode surface. It has been indicated that the experiment results are corresponding with the previous results of the TEM and EIS analysis and well agreeable to the previous literatures[15, 16, 32].

3.5. Effect of pH

Cyclic voltammograms of electroreduction of 2×10^{-4} mol/L nitrofurazone and electrooxidation of 2×10^{-3} mol/L semicarbazide hydrochloride on the Gr/Fe_3O_4/GCE surface at different pH were recorded and the effect of peak current were shown in Figure 6 and Figure 7.

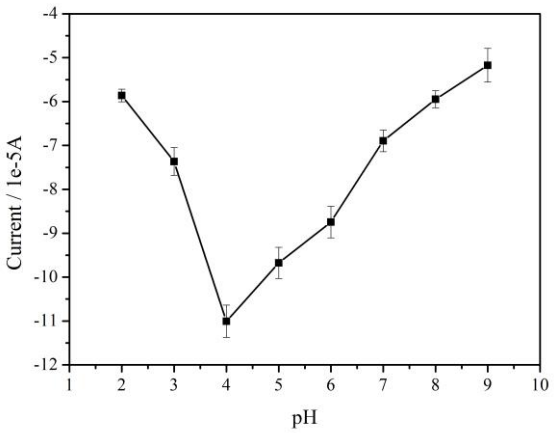

(a)

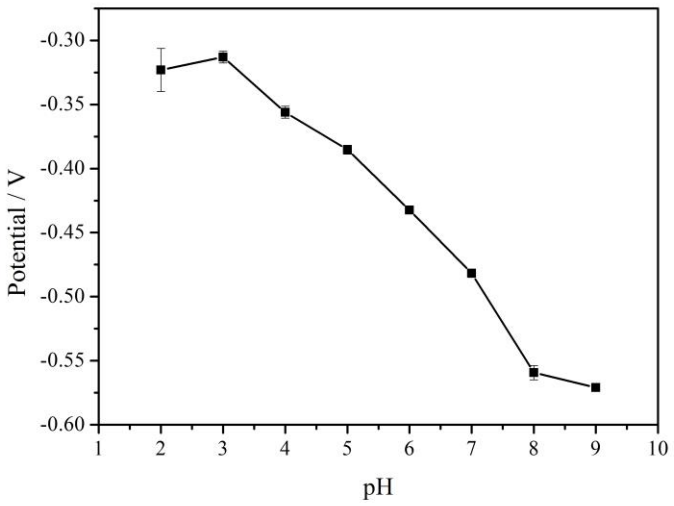

(b)

Figure 6. (a) Effects of the solution pH on the reduction peak current of 2×10^{-4} mol/L nitrofurazone. (b) Relationship with related potential.

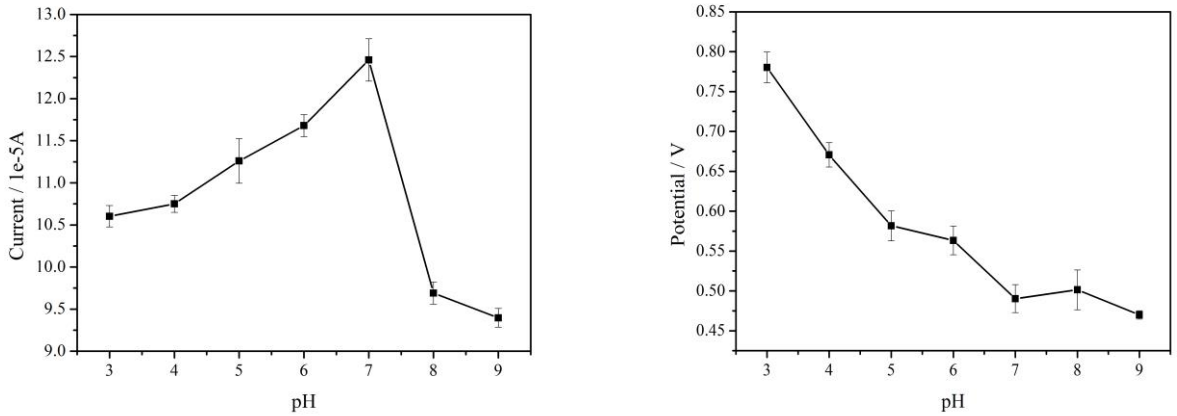

(a) (b)

Figure 7. (a) Effects of the solution pH on the reduction peak current of 2×10^{-3} mol/L semicarbazide hydrochloride. (b) Relationship with related potential.

Upon increasing the solution pH, the peak current of nitrofurazone increased up to 4 and then decreased, and the peak current of semicarbazide hydrochloride increased up to 7 and then decreased. It is especially interesting that the peak potential shifted to a little more negative values upon increasing the solution pH. It could be deduced that the electroreduction process of nitrofurazone and the electrooxidation process of semicarbazide hydrochloride involved protons. Considering all factors, pH 4.0 of nitrofurazone and pH 7.0 of semicarbazide hydrochloride was selected for further studies.

3.6. Effect of scan rates

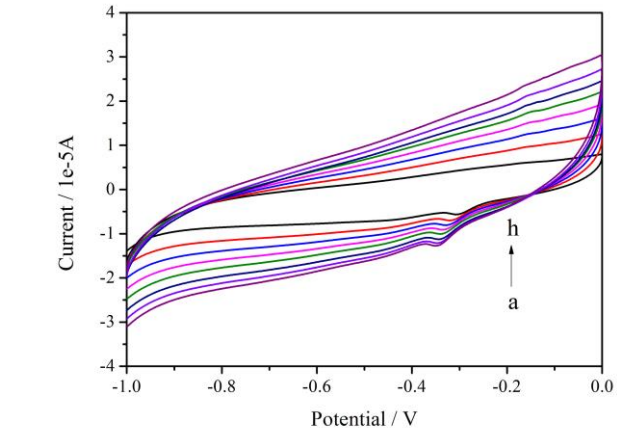

(a)

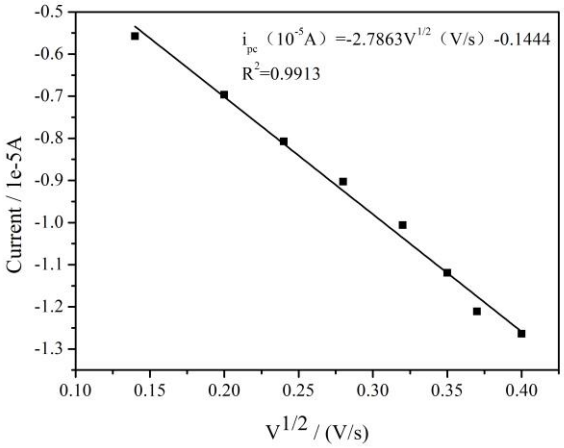

(b)

Figure 8. Cyclic voltammograms of 2×10^{-4} mol/L nitrofurazone on the Gr/Fe_3O_4/GCE in pH 4.0 of Hac-NaAc buffering solution at different scan rates. (a) Curve a to h corresponds to the scan rates： 20 mV/s; 40 mV/s; 80 mV/s; 100 mV/s; 120 mV/s; 140 mV/s; 160 mV/s; (b) Relationship between reduction peak currents and scan rates.

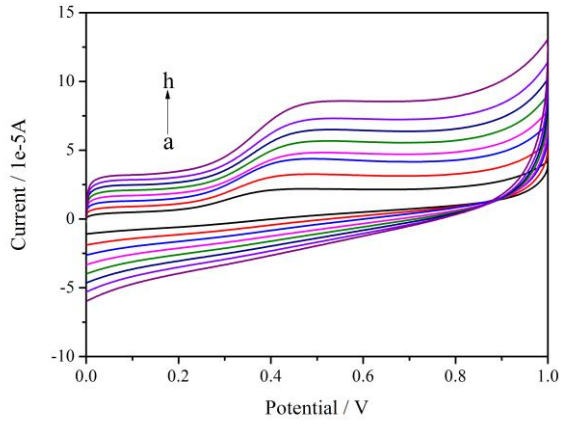

(a)

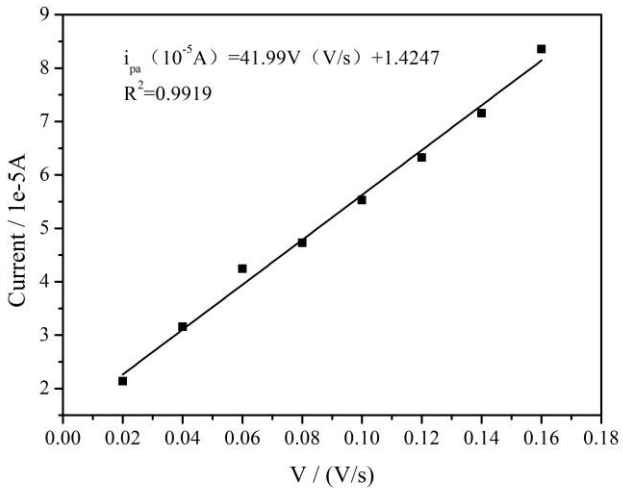

(b)

Figure 9. Cyclic voltammograms of 2×10^{-3} mol/L semicarbazide hydrochloride on the Gr/Fe_3O_4/GCE in pH 7.0 of Hac-NaAc buffering solution at different scan rates. (a) Curve a to h corresponds to the scan rates：20 mV/s; 40 mV/s; 80 mV/s; 100 mV/s; 120 mV/s; 140 mV/s; 160 mV/s. (b) Relationship between oxidation peak currents and the scan rates.

Figure 8 and Figure 9 shows cyclic voltammograms of 2×10^{-4} mol/L nitrofurazone and 2×10^{-3} mol/L semicarbazide hydrochloride recorded at different scan rates from 20 to 160 mV/s. It can be clearly observed that the reduction peak currents was proportional to the square root of the scan rate, with linear equations of ipc（10^{-5}A）=-2.7863 $V^{1/2}$（V/s）-0.1444, R^2=0.9913 and the reduction peak potential was shifted negatively with scan rate in the range from 20-160 mV/s (Figure 7). It represented that the electrochemical reduction of nitrofurazone was a surface diffusion controlled process. We could also see from the above that the oxidation peak currents was proportional to the scan rate, with linear equations of i_{pa}（10^{-5}A）=41.99 V（V/s）+1.4247, R^2=0.9919 and the oxidation peak potential was shifted positively with scan rate in the range from 20-160 mV/s (Figure 8). These results reveal that the electrochemical oxidation of semicarbazide hydrochloride is a typical surface adsorption controlled process.

3.7. Determination of nitrofurazone and semicarbazide hydrochloride concentration

In order to develop a simple determination method for nitrofuranzone and semicarbazide hydrochloride using Gr/Fe_3O_4/GCE, amperometric measurements were performed under stirring conditions and the solution was rapidly homogenized after injection of each drug solution. As shown in Figure 10 and Figure 11, typical amperometric signals obtained on consecutive addition of nitrofuranzone and semicarbazide hydrochloride.

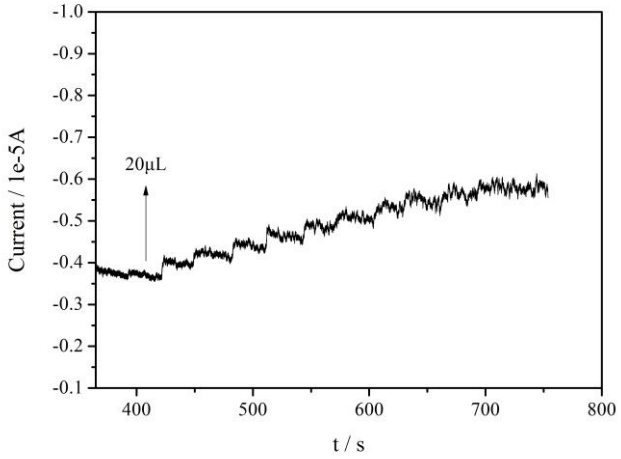

(a)

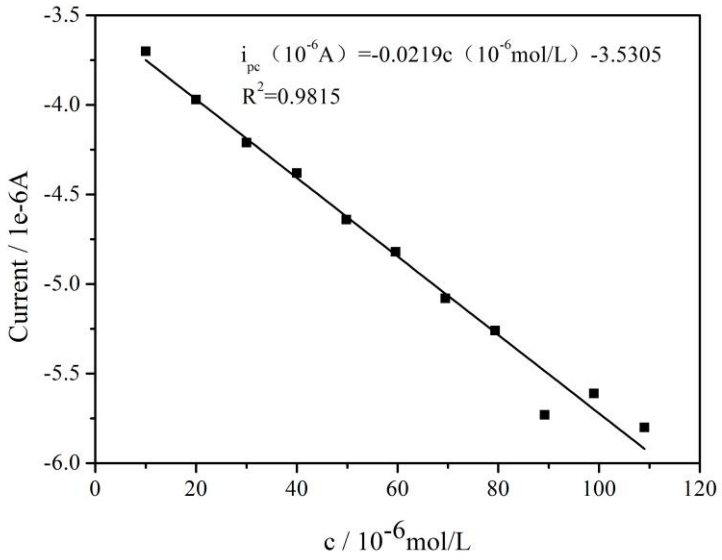

(b)

Figure 10. (a) Typical amperometric signals obtained using Gr/Fe_3O_4/GCE during successive increments of nitrofuranzone to Hac-NaAc buffering solution. (The potential was -0.36 V.) (b) The corresponding calibration curve.

The equation of linear regression for nitrofuranzone was ipc (10^{-6}A)=-0.0219c (10^{-6}mol/L)-3.5303, with the correlation cofficient of 0.9815. The limit of detection was found 2.92×10^{-6} mol/L (signal-to-noise ration =3). The equation of linear regression for semicarbazide hydrochloride was ipa (10^{-6}A)=0.0240c (10^{-6}mol/L) +0.7497, with the correlation cofficient of 0.9992. The limit of detection was found 6.17×10^{-7} mol/L (signal-to-noise ration = 3). The results indicated that the method has low limit, high sensitivity, and can be used for quantitative electrochemical determination of nitrofurazone and semicarbazide hydrochloride.

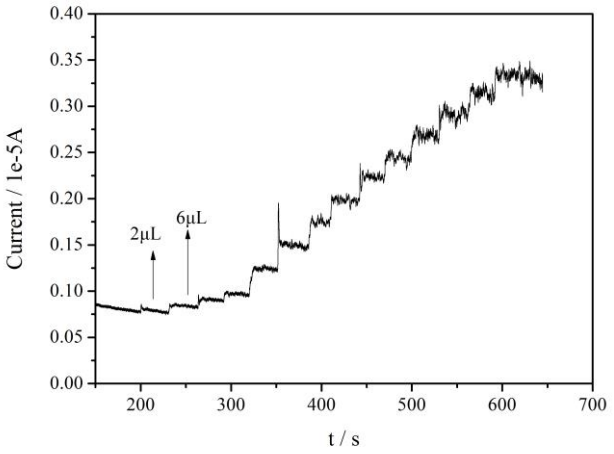

(a)

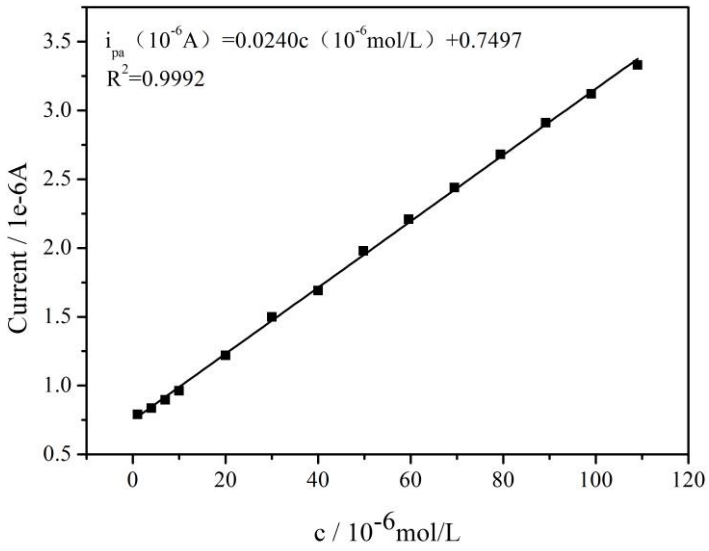

(b)

Figure 11. (a) Typical amperometric signals obtained using Gr/Fe_3O_4/GCE during successive increments of semicarbazide hydrochloride to Hac-NaAc buffering solution. (The potential was 0.60 V). (b) The corresponding calibration curve.

3.8. Influence of coexisting substances

Cyclic voltammetry experiments were carried to investigate the influence of some common metal ions and organic compounds on 2×10^{-4} nitrofurazone and 2×10^{-3} semicarbazide hydrochloride, respectively. Results showed that 100-fold of glucose,fructose,300-fold of K^+, Na^+, Ca^+, Mg^{2+} and 150-fold of Mg^{2+} had no obvious interference on the determination of nitrofurazone and semicarbazide hydrochloride at Gr/Fe_3O_4/GCE(Interference of peak current≤10%).

3.9. Determination of nitrofuranzone and semicarbazide hydrochloride in real samples.

In order to evaluate the feasibility of the proposed modified electrode for real sample detection. The modified electrode was used for the detection of nitrofuranzone residue and semicarbazide hydrochloride residue by standard addition methods in the porks samples. One of them added hydrochloric acid. Then, the two centrifuge tubes were ultrasound for 10 min. Next, the treated centrifuge tubes were centrifuged at 5000 rpm for 10 min. At last, 0.5 mL supernatant was collected and diluted in Hac-NaAc buffering solution. The recovery was investigated by adding different concentration of standard solution. As shown in Table 1, the recoveries are ranged from 80.8%~86.0% and 83.4%~86.1%, respectively, which compared with other method was low[33-34]. This could be because the Pre-treatment was not thorough enough. Raw pork contains too many unknown components, which was not conducive to the extraction of ethyl acetate. In future experiments, the samples should be pretreated with the mixed solution of methanol and water to remove the interfering substances, then added the ethyl acetate to extract the target effectively.

Table 1. Recovery tests of nitrofuranzone and semicarbazide hydrochloride in real samples

nitrofuranzone	Addition (10^{-4} mol/L)	Found (10^{-4} mol/L)	Recovery (%)	RSD (%, n=3)
	4.33	3.50	80.8	3.6
	6.48	5.57	86	4.6
	8.62	7.13	82.7	4.1
semicarbazide hydrochloride	Addition (10^{-4} mol/L)	Found (10^{-4} mol/L)	Recovery (%)	RSD (%, n=3)
	2.17	1.81	83.4	3.7
	4.33	3.73	86.1	5.6
	6.48	5.52	85.2	4.7

4. CONCLUSIONS

In the present study, we have demonstrated nitrofuranzone and semicarbazide hydrochloride both had a sensitive voltammetric response and a novel modified electrode for the detection of nitrofuranzone and semicarbazide hydrochloride was successfully constructed. The Gr/Fe_3O_4/GCE showed significantly improved peak current, higher conductivity and excellent sensitivity over bare GCE, suggesting that the compound material had better electrochemical properties that synthesized via a simple method. Compared with the immunoassay and chromatography mass spectrometry, although the sensitivity of this method had yet to be further improved, it had significant advantages in operation and cost, and made it possible to achieve on-site rapid test. These results reveal that Gr/Fe_3O_4/GCE could be a potential candidate for the electrochemical applications to detect in the real samples.

ACKNOWLEDGMENTS
This work was supported by National Natural ScienceFoundation of China (Grant No. 61301037), Foundation of Henan Educational Committee (Grant No. 13A550194), Key Project of Zhengzhou (Grant No. 20120663), Plan for Scientific Innovation Talent of Henan University of Technology (Grant No. 2012CXRC02), Fundamental Research Funds for the Henan Provincial Colleges and Universities (Grant No. 2014YWQQ05), Youth Backbone Teacher Training Program of Henan University of Technology.

References

1. T. Shoda, K. Yasuhara, M. Moriyasu, T. Takahashi, C. Uneyama , *Archives of Toxicology*, 75 (2001) 297-305.
2. M. Khodari, H. Mansour, Gaber A.M. Mersal, *Journal of Pharmaceutical and Biomedical Analysis*, 20(1999) 579-586.
3. L. Johnston, M. Croft, J. Murby, K. Shearman, *Accreditation and Quality Assurance*, 20 (2015) 401-410.
4. A.A. Abdelwahab, Y. B. Shim, *Sensors and Actuators* B, 221(2015) 659-665.
5. M. B. de la Calle, E. Anklam, *Analytical and Bioanalytical Chemistry*, 382 (2005) 968-977.
6. L. Chen, H. Cui, Y. L. Dong, D. Q. Guo, Y. J. He, X. J. Li, Z. B. Yuan, H. Zou, *Food Analytical* Methods, 9 (2016) 1106-1111.
7. G. O. Noonan, C. R. Warner, W. Hsu, T. H. Begley, G.A. Perfetti, G. W. Diachenko, *Journal of Agricultural and Food Chemistry*, 53(2005) 4680-4685.
8. G.O. Noonan, T. H. Begley, G. W. Diachenko, *Journal of Agricultural and Food Chemistry*, 56(2008) 2064-2067.
9. M. N. Ma, Y. Zhuo, R. Yuan, Y. Q. Chai, *Analytical Chemistry*, 87(2015) 11389-11397.
10. G. L. Li, C. H. Tang, Y. Wang, J. Yang, H. L. Wu, G. Chen, X. J. Kong, *Food Analytical Methods*, 8 (2015) 1804-1811.
11. S. Zhang, Y. M. Guo, Z. Y. Yan, X. M. Sun, X. J. Zhang, *Analytical and Bioanalytical Chemistry*, 407 (2015) 8971-8977.
12. B. S. Sastry, J. V. Rao, T. T. Rao, *Microchimica Acta*, 108 (1992) 185-193.
13. Y. Tang, J. T. X, W. Z. Wang, J. J. Xiang, H.Y. Yang, *European Food Research and Technology*, 232(2011) 9-16.
14. Y. Tang, L. Yan, J. J. Xiang, W. Z. Wang, H. Y. Yang, *European Food Research and Technology*, 232(2011) 963-969.
15. A. Rahi, N. Sattarahmady, R. Dehdari Vais, H. Heli, *Sensor and actuators* B 210(2015) 96-102.
16. I. G. Casella, M. Contursi, *Sensor and actuators* B 209(2015) 25-31.
17. L. Chen, H. Cui, Y. L. Dong, D. Q. Guo, Y. J. He, X. J. Li, Z. B. Yuan, H. Zou, *Food Analytical Methods*, 9 (2016) 1106-1111.
18. C. X. Jiao, C. G. Niu, L. X. Chen, G. L. Shen, R. Q. Yu, *Analytical and Bioanalytical Chemistry*, 376 (2003) 392-398.
19. C. Wang, R. Yuan, Y. Q. Chai, S. H. Chen, F. X. Hu, M. H. Zhang, *Analytica Chimica Acta*, 741 (2012) 15– 20.
20. J. S. Huang, Y. Liu, H. Q. Hou, T. Y. You, *Biosensors and Bioelectronics* 24 (2008) 632–637.
21. T. P. See, A. Pandikumar, H. N. Ming, L. H. Ngee, Y. Sulaiman, *Sensors*, 14(2014) 15227-15243.
22. W. X. Zhang, J. Z. Zheng, J. G. Shi, Z. Q. Lin, Q. T. Huang, H. Q. Zhang, C. Wei, J. H.Chen, S. R. Hu, A. Y. Hao, *Analytica Chimica Acta*, 853 (2015) 285-290.
23. M. A. Farghali, T. A. S. El-Din, A. M. Al-Enizi, R. M. E. Bahnasawy, *International Journal of Electrochemical Science*, 10 (2015) 529-537.
24. O. Akyildirim, H. Medetalibeyoglu, S. Manap, M. Beytur, F. S. Tokali, M. L. Yola, N. Atar, *International Journal of Electrochemical Science*, 10 (2015) 7743-7753.

25. C. J. Fu, G. G. Zhao, H. J. Zhang, S. Li, *International Journal of Electrochemical Science*, 9 (2014)46-60.
26. H. N. Lim, N. M. Zhou, S. S. Lin, I. Harrison, C. H. Chia, *International Journal of Nanomedicine*, 6 (2011) 1817-1823.
27. Y. Li, X. R. Zhao, P. Li, Y. F. Huang, J. Wang, J. M. Zhang, *Analytica Chimica Acta*, 884 (2015) 106-113.
28. S. Erogul, S. Z. Bas, M. Ozmen, S. Yildiz, *Electrochimica Acta*, 186(2015) 302-313.
29. H. Teymourian A. Salimi, S. Khezrian, *Biosensors and Bioelectronics*, 49 (2013) 1-8.
30. S. Chong, G. M. Zhang, H. F. Tian, H. Zhao, *Journal of Environmental Sciences*, 44 (2016) 148-157.
31. Q. Liu, Y. T. Yan, X.W. Yang, J. Qian, J. R. Cai, K. Wang, *Journal of Electroanalytical Chemistry*, 704 (2013) 86-89.
32. V. Climent, A. Rodes, J. M. Orts, J. M. Feliu, A, Aldas, *Journal of Electroanalytical Chemistry*, 436 (1997) 245-255.
33. X. R. Guo, Y. Wang, F. Y. Wu, Y. N. Ni, S. Kokot, *Talanta*, 144(2015) 1036-1043.
34. W. J. Jin, G. J. Yang, H. X. Shao, A. J. Qin, *Sensor and Actuators B*, 188(2013) 271-279.